HDPE-Ash Nanocomposites

E. P. Ayswarya,[1] Beena T. Abraham,[2] Eby Thomas Thachil[1]

[1]*Department of Polymer Science and Rubber Technology, Cochin University of Science and Technology, Kochi, Kerala 682022, India*
[2]*Department of Chemistry, S.N.M. College, Maliankara, 683516 Kerala, India*

Received 17 February 2011; accepted 6 July 2011
DOI 10.1002/app.35191
Published online 20 October 2011 in Wiley Online Library (wileyonlinelibrary.com).

ABSTRACT: Ash-based polymer composites are assuming increasing importance because of the pollutant potential, fine particle size, and low price of ash. Fly ash and rice husk ash are two prominent ash materials on which some investigations have already been done for potential use in polymer composites. This article highlights the results of a study on the use of wood ash in HDPE. Wood ash is mainly a mixture of various metallic compounds and some silica. Here, the characterization of wood ash has been done with the help of XRD, ICPAES, light scattering based particle size analysis, FTIR, and SEM. The results show that wood ash particle size has an average value of 293 nm, much lower than other categories of ash. When blended with HDPE in the presence of a compatibilizer, wood ash gives rise to vastly improved mechanical properties over that of the base polymer. The results prove that wood ash is a valuable reinforcing material for HDPE and the environmental pollution due to wood ash can be solved in a most profitable way by this technique. J Appl Polym Sci 124: 1659–1667, 2012

Key words: nanocomposites; polyethylene (PE); fillers; compatibility; inorganic materials

INTRODUCTION

Polymer nanocomposites consist of a polymeric substance and nanoscale reinforcing materials. These materials show substantial improvements in mechanical properties, gas barrier properties, thermal stability, chemical resistance, dimensional stability, and fire retardancy[1] over the base polymer. The first successful and significant development of polymer nanocomposites was pioneered by Toyota's researchers in the course of developing high performance reinforced plastics applications in automobiles.[2] The important advantages of using polymeric nanocomposites over conventional materials are processing ease, manufacturing versatility, and low overhead production cost.

Composite materials are used in a variety of applications ranging from household appliances to aeronautics. Increasing demand and stringent performance requirements have given an impetus for finding new fillers for the preparation of composites. The polymer industry has a newfound interest in fillers from industrial byproducts and other waste materials having potential recyclability. This new class of fillers includes fillers from natural sources (e.g., natural fibers) and industrial byproducts (e.g., sawdust, rice husk ash, fly ash, and wood ash).[3] These fillers are comparable to commercial fillers such as carbon black, precipitated silica, or talc in particle size. Lower cost while ensuring requisite properties is the prime incentive for their wide acceptance. For improving the compatibility between polar fillers and nonpolar polymers, coupling agents are usually used. These agents modify the interface by interacting with both filler and polymer forming a link between the components.[4] By a union of waste utilization strategies and appropriate blending technology, better and improved composites can be developed simultaneously addressing environmental problems.

Physical properties such as topography, shape, and size are known to affect the reinforcing character of the filler in any matrix[5] Larger particles have lower aggregation tendencies and provide a large volume of stress concentration and aid in increasing impact strength of the composites. On the other hand, smaller particles have higher specific surface area which influences the adsorption characteristics and positively affects the matrix–filler interaction. Most silicate fillers have surface hydroxyl groups (—OH groups) or silanol groups that are hydrophilic in nature and readily absorb moisture from the environment. Most polymers, being hydrophobic and highly viscous, do not wet the filler surface effectively, leading to a poorly formed interface; hence, the need for coupling agents. As an example of filler–matrix interaction, without the use of coupling agents, surface hydroxyl groups are known to

Correspondence to: E. Thomas Thachil (ethachil@cusat.ac.in).

crosslink with epoxy groups of rubber and modify the filler–matrix adhesion by changing the electron accepting or donating character (acid–base character) of the filler. [3]

The preparation of ash-based composites is a growing research area.[6–10] Fly ash is the finely dispersed mineral residue resulting from the combustion of pulverized coal in power plants.[11] Bulk density of fly ash is about 900 kg/m^3 and its particle size ranges from 5 to 70 μm.[12,13] Recently, fly ash has been studied as filler for epoxy resin,[12] thermoplastics (LDPE, HDPE, and PP), and plastic blends (PP/PMMA),[14,15] but studies on its use in rubber are rare. Another type of ash increasingly used as filler in the polymer industry is rice husk ash (RHA).[16] RHA can be black or white depending on how much of the carbon is left unburnt.[17] The predominant component of RHA is silica and is also known as silica ash. White RHA has a smaller surface area (1.4 m^2 g^{-2}) than the black colored one and its particle size is about 50 μm.[3–18]

Wood ash is conventionally used for potash production as a liming agent and a source of nutrients for agricultural plants.[19] It is a cheap and readily available material, crystalline, and thermally stable. Utilization of wood ash in plastic processing is desirable as it can be an environmental nuisance and pollutant where it cannot be used for other applications. To our knowledge, no reports have appeared on the use of this material in polymer processing. Wood ash is hydrophilic, so it suffers from filler-aggregation and moisture absorption. The main problem of preparation of wood ash–thermoplastic composites is the incompatibility between the hydrophilic filler and the hydrophobic polymer which yields composites with poor properties. Major elements present in wood ash are calcium, potassium, and magnesium. Sulfur, phosphorus, and manganese are present at around 1%[19]. Iron, aluminum, copper, zinc, sodium, silicon, and boron are present in relatively smaller amounts. Chemical composition of ash can be determined by Inductively Coupled Plasma Atomic Emission Spectroscopy (ICP-AES).

In the present study, HDPE was used as the matrix and wood ash as reinforcing filler. An attempt has been made to improve the compatibility between wood ash and HDPE by subjecting the polymer to a chemical modification.

EXPERIMENTAL

Materials

High density polyethylene was supplied by Reliance Industries Limited, Mumbai, India. It has a melt flow index of 9.65 g/10 min (190°C/2.16 kg). Maleic anhydride (MA) and dicumyl peroxide (DCP) were supplied by SD Finechem Limited, Mumbai.

Preparation of wood ash

Wood shavings (a mixture of different wood species) were collected from saw mills. They were washed clean with distilled water to remove grit and dried in an oven at a temperature of 100°C for 2 h. They were subsequently burnt in four batches in a muffle furnace for 6 h each at five different temperatures (400°C, 450°C, 500°C, 550°C, and 600°C). This incineration step was found to give concordant values of ash content from the wood waste at each temperature.

Compatibilization

The compatibilizer was the product of a grafting reaction between maleic anhydride (MA) and HDPE with the help of dicumyl peroxide (DCP) initiator at 145°C. The reaction was conducted by melt mixing in a Thermo Haake PolyLab system equipped with roller rotors. About 40 g of HDPE was allowed to melt for 2 min initially. Then varying quantities of MA were added and DCP kept constant. The grafting was done with the rotor speed at 30 rpm and lasted 6 min. Different amounts of MA (0%, 1%, 1.25%, 1.5%, 1.75%, 2%, and 2.5%) were tested to find the optimum percentage.

Preparation of HDPE—Wood ash composites

HDPE was mixed with compatibilizer (Ma-*g*-HDPE) and wood ash in a Thermo Hakke Polylab system earlier mentioned under the same conditions employed for preparing the compatibilizer. Different amounts of the compatibilizer (0%, 5%, 10%, 15%, and 20%) and wood ash (0%, 0.5%, 1%, 1.5%, 2%, and 2.5%) were added and the resulting composites were tested to find optimum percentages.

Preparation of test specimen

The test specimens were prepared from the blends by molding in an electrically heated hydraulic press for 5 min at 150°C under a pressure of 20 MPa. After molding, the samples were cooled down to room temperature under pressure. Rectangular shaped specimens were cut from the molded sheets and used for testing.

Mechanical testing

Mechanical properties were evaluated using Shimadzu Autograph AG-I series Universal Testing Machine at a crosshead speed of 50 mm/min

TABLE I
Particle Size of Different Temperature Ash from XRD Data

Wood ash from different temperatures (°C)	Particle size of wood ash (nm, based on major peaks)
400	182–295
450	180–293
500	177–293
550	174–350
600	174–441

according to ASTM D 882 (2002). Six specimens were used and the average was calculated in each case. These tests provided the ultimate tensile strength, elongation at break, and Young's modulus values of the composites.

Measurement of melt flow index (MFI)

The melt flow indices of HDPE and HDPE–wood ash composites were determined using a CEAST Modular Line Melt Flow Indexer, according to ASTM D1238 (190°C/2.160 kg).

Characterization

Chemical analysis of wood ash

Elemental and chemical compositions of wood ash were obtained using Inductively Coupled Plasma Atomic Emission Spectroscopy (ICPAES). Samples for ICPAES were prepared by first drying the ash in an oven (120°C, 1 h) and then dissolving approximately 100 mg of dried ash in 4 mL of reagent grade, concentrated hydrochloric acid. The mixture was left standing for a couple of hours for complete dissolution. This solution was later diluted to approximately 100 g using distilled, deionized water so that the concentration of various elements was within the linear range of detection for the ICPAE Spectrometer. The solution was analyzed for concentrations of P, K, Ca, Mg, S, Zn, Mn, B, Al, Fe, Si, and Na by Thermo Electron IRIS INTREPID II X SP DUO spectrometer.

Particle size analysis

X-ray diffraction

Samples for X-ray powder diffractometer were first finely ground and then mounted on a glass slide. The sample was analyzed in a Bruker AXS D8 Advance X-Ray powder diffractometer.

Light scattering

The average particle size of wood ash was determined using a particle size analyzer. The sample for particle size analysis was prepared by dissolving 500 mg of wood ash in a 5% solution of potassium oleate and sonicating for 6 h. From this, about 3 mL of solution was used for testing. The solution was analyzed by Malvern Zetasizer (Model Nano-S), manufactured by Malvern Instruments, UK. This instrument works on the principle of light scattering.

Fourier transform infrared spectroscopy

FTIR spectra of representative samples were recorded on a Thermo Nicolet FTIR Spectrometer Model Avatar 370. Samples in the form of thin films, <1 mm thickness, were employed.

Morphology

The morphological characterization of wood ash and tensile fractured surfaces of the composite specimens were carried out using a JEOL Model JSM 6390LV scanning electron microscope. The samples were subjected to gold sputtering prior to electron microscopy to give the necessary conductivity.

RESULTS AND DISCUSSION

Wood ash characterization

From XRD data, using Scherrer's equation,[20] the average particles size of wood ash was found to be

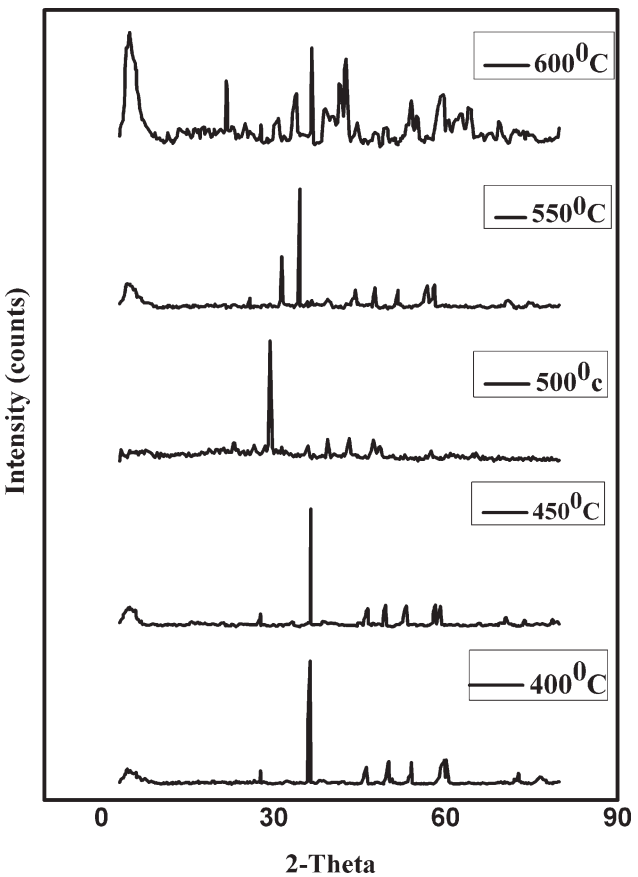

Figure 1 XRD of different temperatures wood ash.

TABLE II
Composition of Wood Ash (ICP-AES) Prepared at 500°C

Component	Weight (%)
Silicon	13.42
Aluminum	3.93
Iron	4.74
Calcium	25.23
Magnesium	36.74
Potassium	10.06
Phosphorous	5.88

234–295 nm. At different temperatures, wood ash shows different particle sizes (Table I). Figure 1 shows the XRD of wood ash at different temperatures. ICPAES (Table II) indicates that wood ash mainly consists of magnesium, calcium, silicon, and potassium. Small amounts of aluminum and iron are also present. Light scattering studies (Table III) reveal that about 0.8% particles are below 100 nm, 43% in the range 100–200 nm, 36.4% in the range 200–300 nm, and 19.7% above 300 nm (upto 615 nm).

Mechanical properties of HDPE—Wood ash nanocomposites

Figure 2 shows the effect of wood ash content on the tensile strength, elongation at break, and Young's modulus of HDPE/wood ash composites. Tensile strength of ash composites decreases steadily with increasing filler loading due to the incompatibility of matrix and filler system. The absence of a coupling agent results in poor adhesion of the ash particulates to the matrix. Weak interfacial regions imply that the filler particles cannot carry any of the load applied to the composites and the entire stress has to be carried solely by the matrix material.[18] If the filler particles are not wetted by the matrix polymer, the filler particles and agglomerates get filled with air, introducing porosity to the internal structure of

TABLE III
Particle Size of Wood Ash (500°C) from Light Scattering

Wood ash particle size (nm)	Mean volume (%)
78.882	0.2
91.28	0.6
105.7	2.7
122.4	6.1
141.8	9.2
164.2	11.6
190.1	13.4
220.2	13.5
255	12.4
295.3	10.7
342	8.7
396.1	6.2
458.7	3.4
531.2	1.2
615.1	0.2

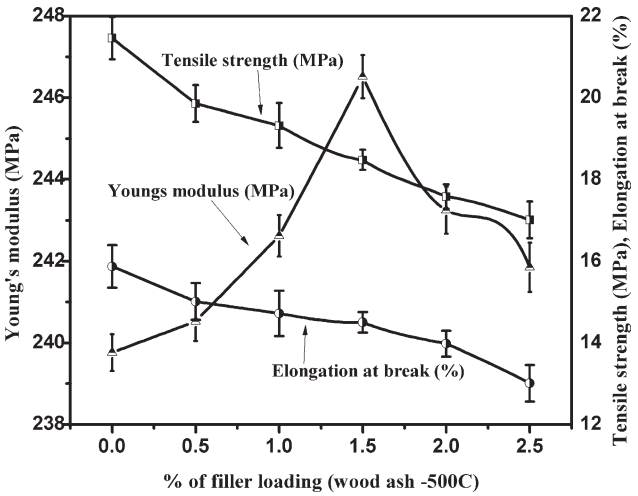

Figure 2 Tensile strength, elongation at break, and Young's modulus versus % filler loading in HDPE.

the composites that leads to an adverse effect on the tensile strength. Elongation at break predictably decreases with increasing filler loading. The poor bonding of the filler particles to the polymer does not permit HDPE to attain full elongation. Young's modulus increases with increasing filler loading up to 1.5% and then decreases. Such behavior from incompatible filler materials is well known.[21–23]

Figure 3 shows the effect of MA content while preparing the compatibilizer, MA-*g*-HDPE, in the presence of a constant amount of a free radical initiator, DCP. The variation in tensile strength is not substantial. The maximum tensile strength occurs at 2% MA loading. Elongation at break initially increases but decreases with more MA. Young's modulus shows an increasing tendency with MA loading. The scheme of reaction shown below (Scheme 1) illustrates the changes undergone by the HDPE chain. The anhydride ring attached to

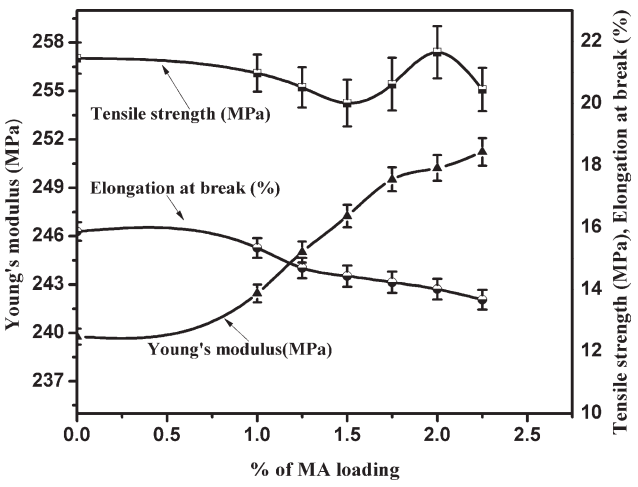

Figure 3 Tensile strength, elongation at break, and Young's modulus versus % MA content in MA-*g*-HDPE.

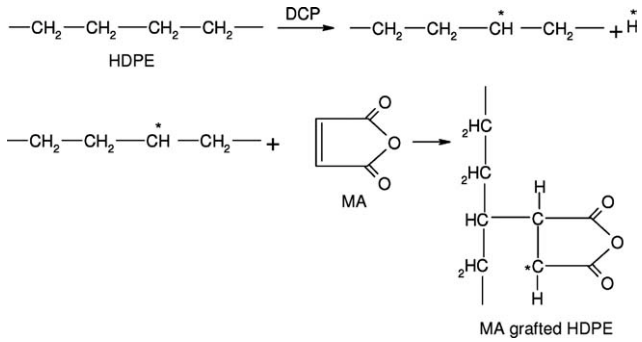

Scheme 1 Formation of compatibilizer.

the polymer chain does not allow HDPE polymer molecules to slip over one another easily. The mechanical property changes mentioned above are a direct consequence of this.

Figure 4 is a plot of the effect of compatibilizer % on tensile strength, elongation at break, and Young's modulus of unfilled HDPE. There is some dependence of compatibilizer content on tensile strength. The tensile strength increases with increasing percentage of compatibilizer up to 15% and then decreases. This figure shows that elongation at break also displays a maximum with respect to compatibilizer % but at a different value. Apparently, at higher loadings of compatibilizer, the presence of too many anhydride rings only serves to make the blend less homogeneous and poor in mechanical strength. Young's modulus increases steadily with increasing percentage of compatibilizer as the straightening of polymer chains becomes more difficult by the presence of the bulky anhydride group.

Figure 5 shows the effect of different temperature of incineration of wood ash on the tensile strength, elongation at break, and young's modulus of compatibilized HDPE. The tensile strength shows a maximum at an ash incineration temperature of 500°C and an ash concentration of 1.5% (kept constant). The XRD data (Table I) establish that the particle size at 500°C is the lowest for wood ash. The high tensile strength may be based on this. The elongation at break also shows a maximum at 500°C. The modulus does not exhibit a strong dependence on the incineration temperature. Further studies were done using the ash prepared at 500°C.

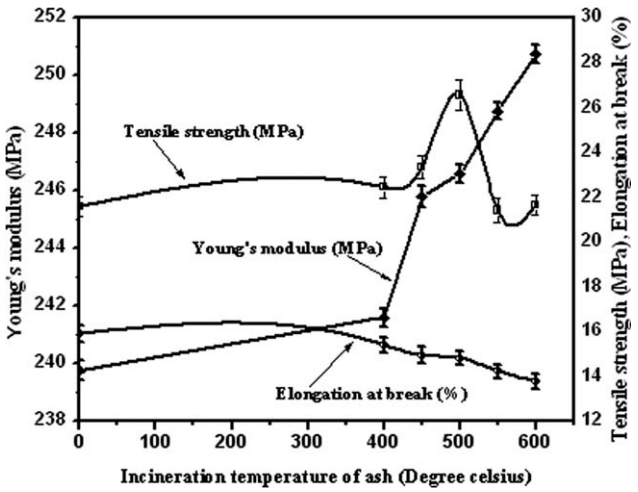

Figure 5 Tensile strength, elongation at break, and Young's modulus versus incineration temperature of ash in compatibilized HDPE.

The tensile strength of the compatibilized HDPE-ash composite increases with increasing percentage of filler loading (Fig. 6). The behavior of the composite in the presence of the compatibilizer is vastly different. At 1.5% ash the improvement in tensile strength is as much as 20%. The use of the compatibilizer has proven to be effective in enhancing the dispersion, adhesion, and compatibility of the filler

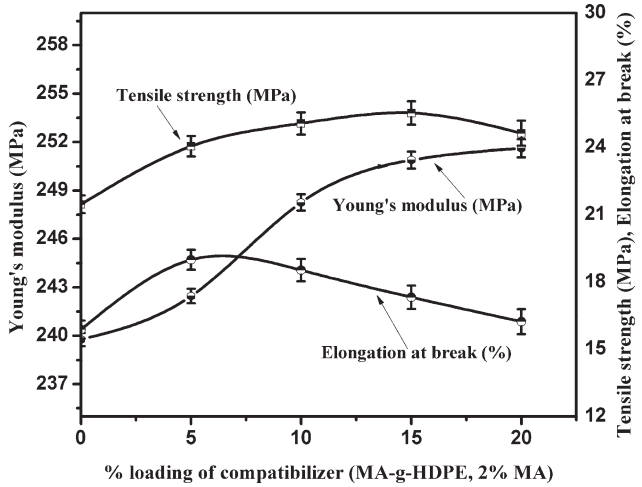

Figure 4 Tensile strength, elongation at break, and Young's modulus versus % of compatibilizer in HDPE.

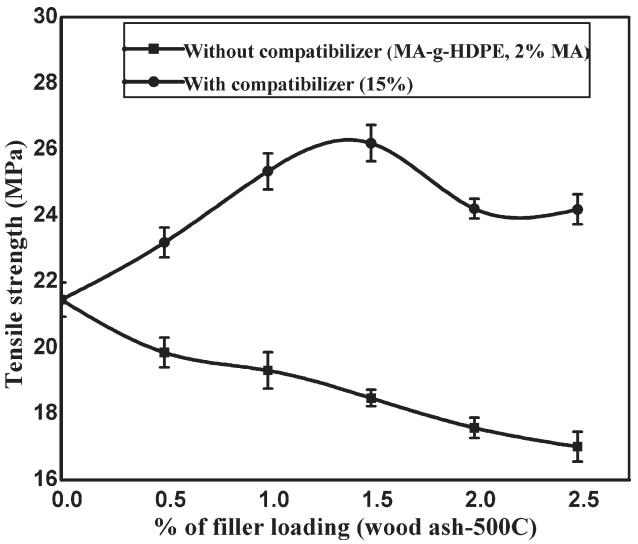

Figure 6 Tensile strength versus % of filler in compatibilized HDPE.

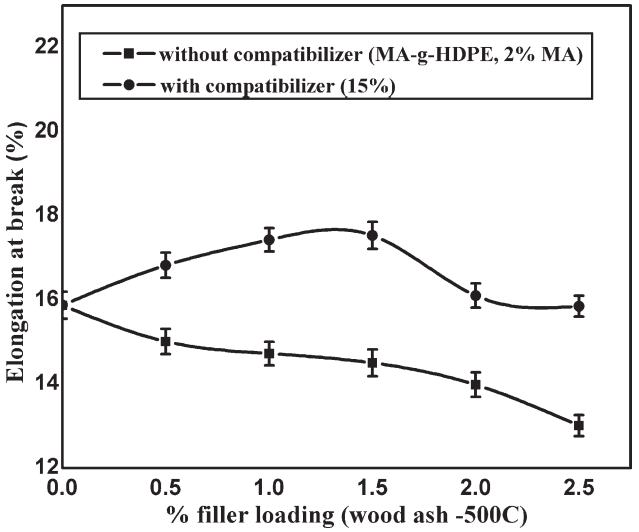

Figure 7 Elongation at break versus % of filler in compatibilized HDPE.

with the hydrophobic matrix. Figure 7 shows that the breaking elongation of the composite also reaches a maximum at 1.5 wt % of ash. When the composites are under exterior stress, the filler helps to distribute the stress evenly and delay the rupture of the material. Figure 8 shows that Young's modulus of the composites increases with increasing filler loading. The interfacial adhesion is increased by the presence of the compatibilizer and the high surface area of the filler gives rise to increased modulus and strength.

Melt flow measurement

The melt flow index is one of the most common parameters specified when describing a thermoplastic polymer. Figures 9–13 show the variation of the

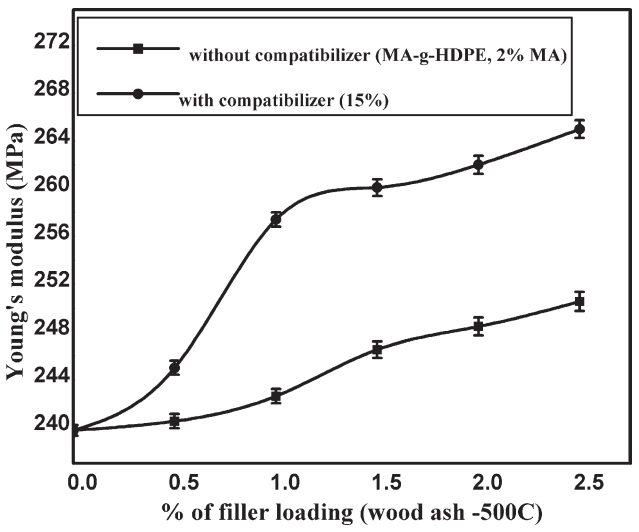

Figure 8 Young's modulus versus % of filler in compatibilized HDPE.

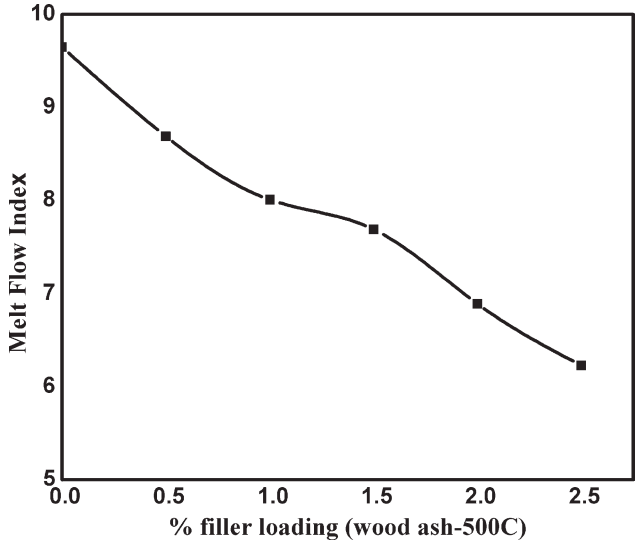

Figure 9 Melt flow index versus % filler in noncompatibilized HDPE.

melt flow index of HDPE in the presence of filler and compatibilizer. Addition of compatibilizer was expected to increase the viscous as well as elastic response of the system by improving the filler matrix interaction. In all the five cases shown, the melt flow index values decrease with loading of filler and compatibilizer. Low melt flow index indicates a higher melt viscosity.[24] The melt flow index indicates the degree of chain entanglement of polymer chains by chemical or physical crosslinks. The ash particles are instrumental in increasing the entanglement between polymer chains.

FTIR measurements

FTIR spectroscopy is very useful for studying the interaction of the polymer with compatibilizer and

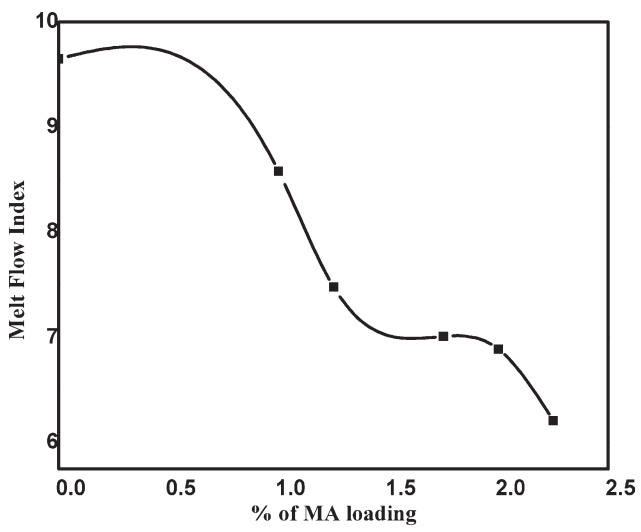

Figure 10 Melt flow index versus % MA content in MA-g-HDPE.

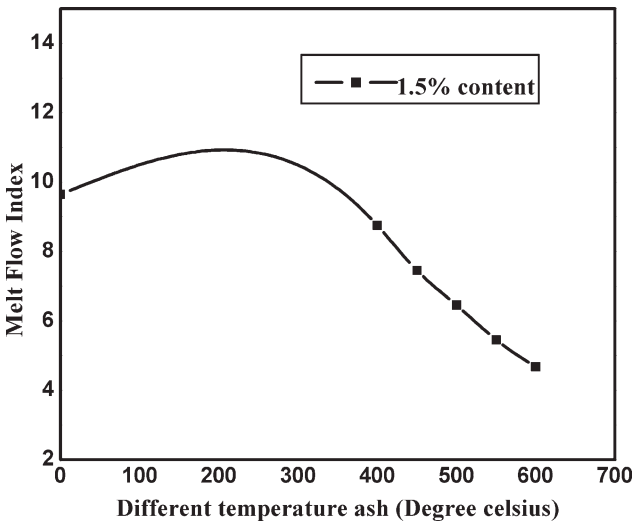

Figure 11 Melt flow index versus % different temperature ash in compatibilized HDPE.

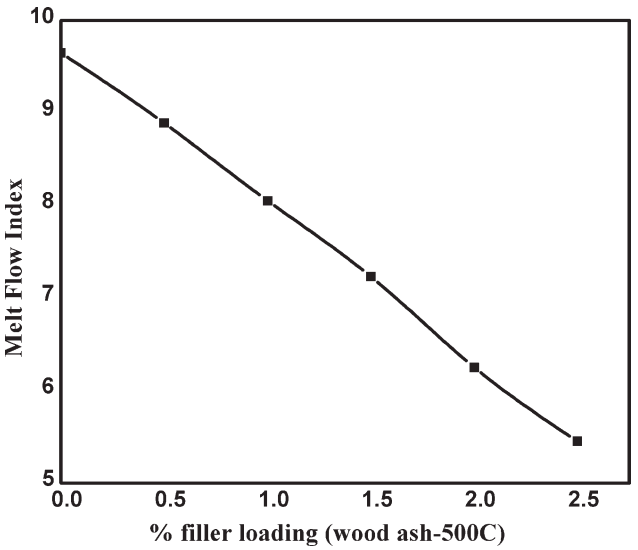

Figure 13 Melt flow index versus % filler in compatibilized HDPE.

filler. Figures 14 and 15 show the spectra of wood ash and compatibilized HDPE-wood ash composites. The FTIR spectrum of wood ash shows a peak at 1093 cm^{-1} corresponding to Si—O—Si stretching vibration.[20] The peak at 875–550 cm^{-1} shows vibration of Al_2O_3.[10] The peak at 3423.83 cm^{-1} indicates the presence of O—H group in the wood ash.[20] The spectrum of the compatibilized composite shows a peak at 1740 cm^{-1} assignable to symmetric stretching of C=O group present in ester moieties. This result indicates that the functional groups of MA-*g*-HDPE can react with the hydroxyl groups of wood ash, leading to covalent bonding and possible esterification reactions.[25]

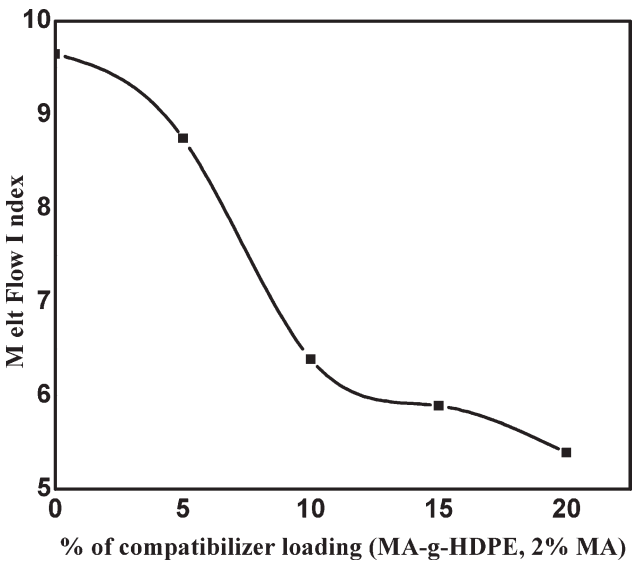

Figure 12 Melt flow index versus % of compatibilizer in HDPE.

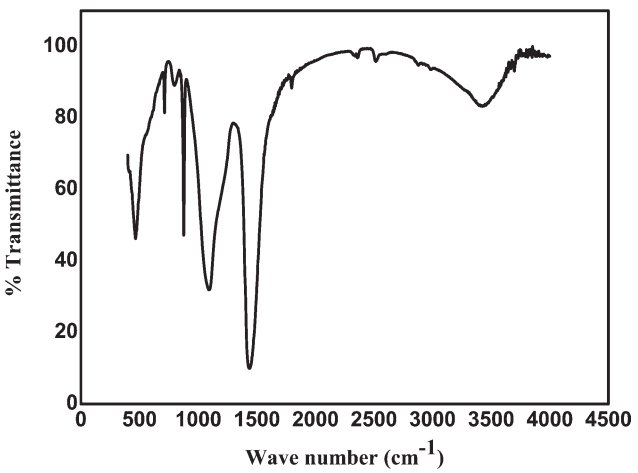

Figure 14 FTIR of wood ash.

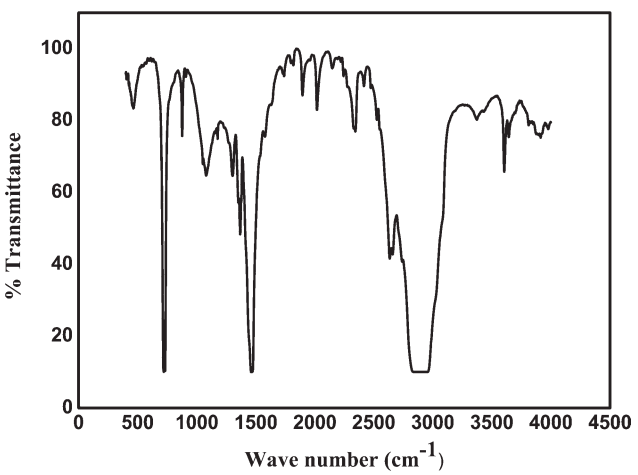

Figure 15 FTIR of composite.

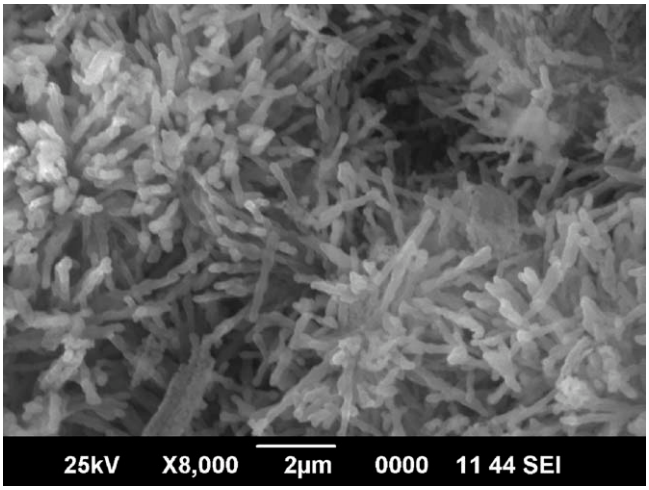

Figure 16 SEM micrographs of wood ash (500°C).

Scanning electron microscopy (SEM)

Figure 16 shows that wood ash particles have a rough cylindrical shape with a tendency to agglomerate. A micrograph of the failure surface of wood ash filled-HDPE without MA-*g*-HDPE is shown in Figure 17. Wood ash particles in the composite are found to be of widely different sizes possibly due to agglomeration, poor wetting, and a nonhomogenous dispersion. Under these conditions, the mechanical properties of the uncompatibilized HDPE–wood ash composites are understandably poor. Figure 18 is a micrograph of the surface of the wood ash filled-HDPE composites compatibilized by MA-*g*-HDPE. The presence of MA-*g*-HDPE leads to a homogenous dispersion of wood ash and improved wettability. The failure surface shows signs of greater energy absorption by the presence of undulations and a wavy texture. Hence the superior properties.

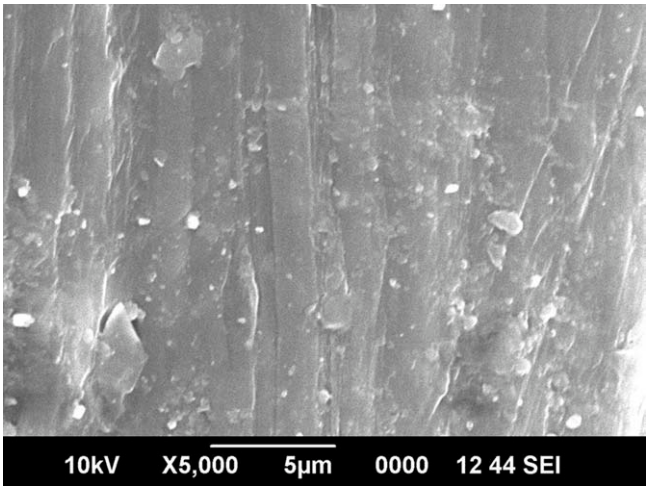

Figure 17 SEM micrographs of wood ash (500°C) filled HDPE.

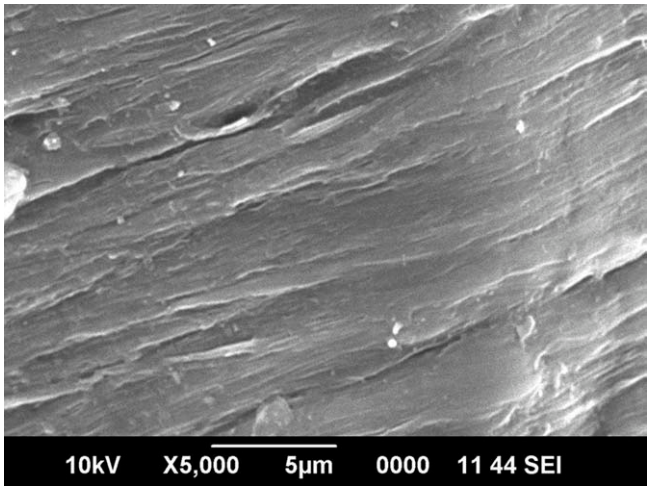

Figure 18 SEM micrographs of wood ash (500°C) filled compatibilized HDPE.

CONCLUSIONS

Wood ash mainly consists of aluminum, iron, calcium, magnesium, potassium, phosphorous, and silicon compounds. The average particle size of wood ash is 293 nm. Wood ash can be incorporated into HDPE by the melt blending process. Incompatibility between HDPE and wood ash leads to deterioration of composite properties. A compatibilizer consisting of MA-*g*-HDPE can greatly improve the performance of wood ash–HDPE composites. Interaction between metal oxide/hydroxides and anhydride rings enhances the properties of wood ash–HDPE composites. There is considerable improvement in the mechanical properties of HDPE by the incorporation of wood ash. The best mechanical properties are observed at 1.5% wood ash. The method provides a means to utilize ash, a pollutant, to gainfully improve the properties of HDPE.

References

1. Emmanuel, P. G. Appl Organometal Chem 1998, 12, 675.
2. Kojima, Y.; Usuki, A.; Kawasumi, M.; Okada, A.; Kurauchi, T.; Kamigaito, O. J Polym Sci Part A Polym Chem 1993, 31, 983.
3. Chaudhary, D. S.; Jollands, M. C.; Cser, F. Silicon Chem 2002, 1, 281.
4. Mazaid, N. A.; EL-Nashar, D. E.; Sadek, E. M. J Mater Sci 2009, 44, 2665.
5. Nakamura, Y.; Okabe, S.; Lida, T. Polym Polym Compos 1999, 7, 177.
6. Nittaya T.; Apinon, N.; Chiang, M. J Sci 2008, 35, 206.
7. Da Dosta, H. M.; Visconte, L. L. Y.; Nunes, R .C. R.; Furtado, C. R. G. J Appl Polym Sci 2002, 83, 2331.
8. Ana A.; Santiago, G. P.; Abad, M. J.; Cano, J.; Barral, L. Rheol Acta 2010, 49, 607.
9. Wong, K. W. Y.; Truss, R. W. Compos Sci Technol 1994, 52, 361.
10. Najib, N. N.; Ismail, H.; Azura, A. R. Polym Plast Technol Eng 2009, 48, 1062.

11. Dazuo, C.; Selic, E.; Herbell, J.-D. J Zhejiang Univ Sci A 2008, 9, 681.
12. Kulkarni, S. M.; Kishore, J. J Mater Sci 2002, 37, 4321.
13. Deb Nath, D. C.; Sri Bandyopadhyay, T. D.; Yu, A.; Zeng, Q.; Blackburn, D.; White, C. J Mater Sci 2009, 44, 6078.
14. Wang, M.; Shen, Z.; Cai, C.; Ma, S.; Xing, Y. J Appl Polym Sci 2004, 92, 126.
15. Jarvela, P. A.; Jarvela, P. K. J Mater Sci 1996, 31, 3853.
16. Fuad, M. Y. A.; Shukor, R.; Isak, Z. A. M.; Omar, A. K. M. Plast Rubber Comp Process Appl 1994, 21, 225.
17. Ishak, Z. A. M.; Bakar, A. A. Eur Polym J 1995, 31, 259.
18. Ismail, H.; Mega, L.; Abdul Khalil, H. P. S. Polym Int 2001, 50, 606.
19. Misra, M. K.; Ragland, K. W.; Baker, A. J. Biomass Bioenergy 1993, 4, 103.
20. Thomas Paul, K.; Satpathy, S. K.; Manna, I.; Chakraborty, K. K.; Nando, G. B. Nanoscale Res Lett 2007, 2, 397.
21. Ismail, H.; Mohamad, Z.; Baker, A. A. Polym Plast Technol Eng 2003, 42, 81.
22. Bose, S.; Mahanwar P. A. J Mineral Mater Characteris Eng 2004, 3, 65.
23. Jayasree, T. K.; Predeep, P. J Elastomer Plast 2008, 40, 127.
24. Stabi, K. J.; Suchon, L.; Rojek, M.; Scczepanik, M. J Achiev Mater Manufact Eng 2009, 33, 149.
25. Kim, H.-S.; Lee, B.-H.; Choi, S.-W.; Kim, S.; Kim, H.-J. Compos Part A 2007, 38, 1478.